Available online at www.sciencedirect.com
ScienceDirect
Bioorganic & Medicinal Chemistry 16 (2008) 2886–2893
Bioorganic & Medicinal Chemistry

Biocatalytic and semisynthetic optimization of the anti-invasive tobacco (1*S*,2*E*,4*R*,6*R*,7*E*,11*E*)-2,7,11-cembratriene-4,6-diol

Khalid A. El Sayed,[a,*] Surat Laphookhieo,[a] Hany N. Baraka,[a] Muhammad Yousaf,[a] Anne Hebert,[a] Danielle Bagaley,[b] Frederick A. Rainey,[b] A. Muralidharan,[a] Shibu Thomas[a] and Girish V. Shah[a]

[a]*Department of Basic Pharmaceutical Sciences, College of Pharmacy, University of Louisiana at Monroe, 700 University Avenue, Monroe, LA 71209, USA*
[b]*Department of Biological Sciences, Louisiana State University, Baton Rouge, LA 70803, USA*

Received 24 November 2007; revised 27 December 2007; accepted 28 December 2007
Available online 3 January 2008

Abstract—Tobacco cembranoids were reported to inhibit tumorigenesis. Biocatalysis of (1*S*,2*E*,4*R*,6*R*,7*E*,11*E*)-2,7,11-cembratriene-4,6-diol (**1**) using the symbiotic *Bacillus* sp. NC5, *Bacillus* sp. NK8, and *Bacillus* sp. NK7, isolated from the Red Sea sponge *Negombata magnifica*, afforded two new and four known hydroxylated metabolites **3**–**8**. The use of symbiotic marine bacteria as biocatalysts for bioactive natural product scaffolds is very rare. Cembranoid **1** carbamate analogs **9**–**11** were prepared by its reaction with corresponding isocyanates. Cembranoid **1** and its bioconversion and carabamate products show anti-invasive activity against the human highly metastatic prostate PC-3M cancer cell line at 10–50 nM doses in Matrigel assay.

1. Introduction

The leaf and flower cuticular wax of most *Nicotiana* species contain high amounts of cembranoid diterpenes.[1] Cembranoids possess 14-membered macrocyclic rings substituted by an isopropyl residue at C-1 and by three symmetrically disposed methyl groups at positions C-4, C-8, and C-12. The two epimeric tobacco cembranoids (1*S*,2*E*,4*R*,6*R*,7*E*,11*E*)-2,7,11-cembratriene-4,6-diol (**1**) and its C-4 epimer were among the earliest reported.[1–4] The structure and absolute stereochemistry of **1** was based on X-ray crystallography.[1–3] Both cembranoids are key flavor ingredients in tobacco.[1,2] Biodegradation of **1** and its epimer during flue-cured fermentation of tobacco leaves produces a range of flavor compounds.[1,2,5]

Tobacco cembranoids exert a wide range of bioactivity. They block the expression of the behavioral sensitization to nicotine and inhibit neuronal acetylcholine receptors in rats, suggesting a possible use of these compounds for the treatment of nicotine addiction.[6] Tobacco cembranoids also show insecticidal, prostaglandin, plant growth, and fungal spore germination inhibitory activities.[1,2,5,7] Cembranoid **1** and its C-4 epimer from cigarette smoke condensate were reported as anticancer ingredients in 1985.[8] Later, both cembranoids were reported to inhibit the induction of Epstein–Barr virus (EBV) early antigen by the phorbol ester, 12-*O*-tetradecanoylphorbol-13-acetate (TPA), in lymphoblastoid Raji cells.[9] They also inhibited the induction of ornithine decarboxylase (OD) activity by TPA in the mouse epidermis and inhibited the promotional effects of TPA on skin tumor formation initiated by 7,12-dimethylbenz[*a*]anthracene (DMBA) in mice.[10]

Biocatalysis is the use of growing microbial cultures, enzymes, or immobilized cells to enhance the bioactivity of a starting material through induction of stereospecific reactions.[12–14] Although biocatalysis has been used to generate new chiral derivatives and increase the efficacy of drugs by metabolic activation is well documented, the use of marine microorganisms as biocatalysts for a bioactive natural product scaffold has been rarely reported.[12–16]

Keywords: Tobacco cembranoids; Biocatalysis; Symbiotic marine microbials; Semisynthesis; Anti-invasive.
* Corresponding author. Tel.: +1 318 342 1725; fax: +1 318 342 1737; e-mail: elsayed@ulm.edu

0968-0896/$ - see front matter © 2008 Elsevier Ltd. All rights reserved.
doi:10.1016/j.bmc.2007.12.056

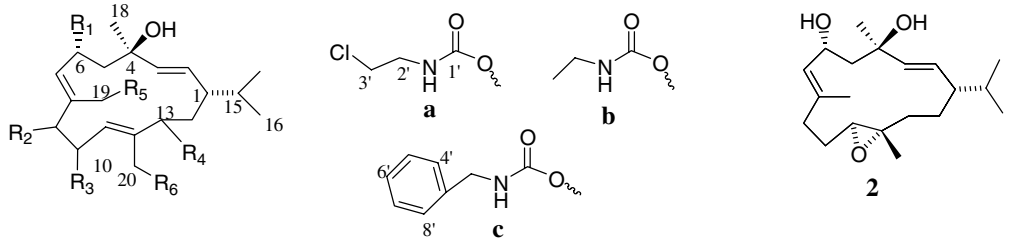

	R_1	R_2	R_3	R_4	R_5	R_6
1	OH	H	H	H	H	H
3	OH	H	H	H	OH	H
4	OH	β-OH	H	H	H	H
5	OH	H	H	H	H	OH
6	OH	H	α-OH	H	H	H
7	OH	H	β-OH	H	H	H
8	OH	H	H	α-OH	H	H
9	a	H	H	H	H	H
10	b	H	H	H	H	H
11	c	H	H	H	H	H

Studies examining the biotransformation of **1** and its epimer started in 1987, mainly to generate flavor-enhancers that can be added to tobacco during its fermentation.[2,3,11,12] The terrestrial bacterium *Bacillus megaterium* NH5 bioconverted tobacco cembranoids to C-10- and C-20 hydroxy analogs, improving the tobacco natural odor and taste and reducing its irritating effects on the throat and lungs.[12,17,18] Plant cell cultures *Tripterygium wilfordii* and *Nicotiana sylvesteris* also biotransformed **1**, its C-4 epimer, and other minor tobacco cembranoids.[12,19–21] These reactions mainly afforded **2**, the 11*S*, 12*S* epoxide analog of **1**, the epoxide analog, and several minor 10-, 12-, and 13-enzymatically hydroxylated and rearranged triols of the C-4 epimer of **1**.[12,19–21]

There is a single report on the structure–activity relationship study aimed to optimize the anticancer activity of tobacco cembranoids.[10] Esterification of C-6 of **1** and its C-4 epimer using acetic, propionic, butyric, valeric, and benzoic acid anhydrides reduced the activity in the Epstein–Barr virus early antigen induction model by increasing the IC_{50} values and cytotoxicity, suggesting the importance of a free C-6 hydroxy group for the activity.[10] Cytotoxicity increased with the increase of acyl carbon number.[10] Oxidation of C-6 alcohol of **1** and its C-4 epimer to β-hydroxyketones slightly reduced the activity by increasing the IC_{50}, which further confirmed the importance of a hydrogen bonding donor pharmacophore at C-6.[10,12] The purpose of the present study is to optimize the anticancer activity of **1** using biocatalytic and semisynthetic approaches.

Biocatalysis was conducted with the use of several novel symbiotic marine bacteria. Semisynthetic carbamoylation of C-6 in **1** targeted the addition of more hydrogen bonding donor and acceptor pharmacophores at this key position to enhance the binding affinity of the products toward its target protein(s).

2. Results and discussion

High amounts of tobacco α- and β-2,7,11-cembratriene-4,6-diols were isolated from fresh *Nicotiana tabacum* leaf powder. Their identification was based on extensive analyses of their NMR data and comparison with the literature.[1–3,11] Several symbiotic bacteria were cultured and isolated from the Red Sea sponge *Negombata magnifica*. The identity of the bacteria was revealed by 16S rRNA sequence analysis.[22] Thirty growing symbiotic bacterial species were screened for their ability to bioconvert **1**. Of these, *Bacilli* species NC5, NK8, and NK7 were selected for the scale-up bioconversion. This selection was based on the TLC diversity of the generated metabolites.

Biocatalysis of **1** using *Bacillus* sp. NC5 afforded two new hydroxylated metabolites **3** and **4**, along with the known metabolites (1*S*,2*E*,4*R*,6*R*,7*E*,11*Z*)-2,7,11-cembratriene-4,6,20-triol (**5**) and (1*S*,2*E*,4*R*,6-*R*,7*E*,11*E*,10*R*)-2,7,11-cembratriene-4,6,10-triol (**6**).[5,23] Fermentation of **1** for 14 days, using *Bacilli* species NK7 and NK8 afforded the known (1*S*,2*E*,4*R*,6-*R*,7*E*,11*E*,10*S*)-2,7,11-cembratriene-4,6,10-triol (**7**) and (1*S*,2*E*,4*R*,6*R*,7*E*,11*E*,13*R*)-2,7,11-cembratriene-4,6,13-triol (**8**), respectively.[5,23]

The HREIMS of metabolite **3** showed a molecular ion peak at *m*/*z* 345.2406 $[M+Na]^+$ corresponding to the molecular formula $C_{20}H_{34}O_3$. The ^1H and ^{13}C NMR data (Table 1) suggested a monohydroxy derivative of **1**. The methylene proton signals at δ 3.57 (d, $J = 11.1$ Hz) and δ 3.51 (d, $J = 11.1$ Hz) were assigned for the newly oxygenated C-19 (Table 1). They showed a ^3J-HMBC correlation with the olefinic methine carbon C-7 (δ 130.2). Proton H-7 in turn showed a COSY correlation with the oxygenated methine H-6 (δ 4.82), confirming the assignment of segment C-6/C-8. The methylene H_2-19 also showed a ^3J-HMBC correlation with the methylene C-9 (δ 38.0). Thus, metabolite **3**

Table 1. ^{13}C and ^{1}H NMR Data of Metabolites **3**–**4**[a]

Position	**3**[a]		**4**[a]	
	δ_C	δ_H	δ_C	δ_H
1	47.5, CH	1.63, m	46.5, CH	1.51, m
2	131.8, CH	5.24, ddq (15.8, 8.8, 1.8)	131.8, CH	5.21, dd (15.8, 8.8)
3	137.3, CH	5.40, d (15.8)	136.3, CH	5.35, d (15.8)
4	72.1, qC	—	71.5, qC	—
5	52.2, CH_2	2.15, m 1.95, m	52.2, CH_2	2.00, m 1.88, m
6	64.4, CH	4.82, dd (9.8, 9.0)	64.4, CH	4.86, dd (9.6, 9.2)
7	130.2, CH	5.47, d (9.8)	126.4, CH	5.62, d (9.9)
8	136.2, qC	—	133.2, qC	—
9	38.0, CH_2	2.25, m, 2.20, m	70.9, CH	4.23, brs
10	22.5, CH_2	2.33, 2H, m	38.1, CH_2	2.40, m 2.32, m
11	128.0, CH	5.28, m	124.7, CH	4.99, brt (3.6)
12	136.2, qC	—	136.8, qC	—
13	27.9, CH_2	2.27, m, 1.90, m	27.9, CH_2	2.04, m, 1.66, m
14	32.0, CH_2	1.42, 2H, m	32.0, CH_2	1.40, m 1.31, m
15	32.8, CH	1.51, m	32.8, CH	1.51, m
16	19.2, CH_3	0.79, 3H, d (6.6)	19.2, CH_3	0.78, 3H, d (6.6)
17	20.7, CH_3	0.84, 3H, d (6.6)	20.7, CH_3	0.81, 3H, d (6.6)
18	28.9, CH_3	1.39, 3H, s	28.9, CH_3	1.41, 3H, s
19	60.0, CH_2	3.57, d (11.1), 3.51, d (11.1)	15.1, CH_2	1.53, 3H, s
20	16.1, CH_3	1.76, 3H, s	16.1, CH_3	1.69, 3H, s

[a] In $CDCl_3$, 400 MHz for ^{1}H and ^{13}C NMR. Coupling constants (*J*) are in Hz.

was proved to be (1*S*,2*E*,4*R*,6*R*,7*Z*,11*E*)-2,7,11-cembratriene-4,6,19-triol.

The HREIMS, ^{1}H, and ^{13}C NMR data (Table 1) data of metabolite **4** also suggested a monohydroxy derivative of **1**. The oxygenated broad singlet at δ 4.23, which correlated with a methine carbon at δ 70.9, was assigned for the newly oxygenated C-9 (Table 1). Carbon C-9 showed a ^{3}J-HMBC correlation with the methyl proton singlet H_3-19 (δ 1.53). Proton H-9 showed COSY correlations with H_2-10 multiplets (δ 2.40 and 2.32), which in turn showed COSY correlations with the olefinic methine broad triplet H-11 (δ 4.99), confirming the assignment of the segment C-9/C-11. The relative stereochemistry of 9-hydroxy group was assigned based on NOESY data. The α-oriented H_3-18 (δ 1.41) showed a NOESY correlation with H-9, suggesting a similar relative stereochemistry. Thus, the 9-hydroxy group should be β-oriented and therefore, metabolite **4** was found to be (1*S*,2*E*,4*R*,6*R*,7*E*,9*S*,11*E*)-2,7,11-cembratriene-4,6,9-triol.

Reflux of **1** in toluene with chlororethyl, ethyl, and benzyl isocyanates, in presence of catalytic amount of triethylamine, afforded the C-6 carbamates **9**–**11**, respectively.[24] The HRMS analysis of compound **9** revealed the molecular formula, $C_{23}H_{38}ClNO_3$, with M and M+2, 3:1, isotopic clusters characteristic of a monochlorinated compound. The downfield shifting of C-6 carbon chemical shift in **9** (+4.9 ppm), compared with that of the starting material **1**, confirmed carbamoylation at this position. The ^{1}H and ^{13}C NMR data (Table 2) further supported this fact. The carbonyl carbon at δ 156.5 was assigned C-1′. This was based on its ^{3}J-HMBC correlation with the methylene multiplet H_2-2′ (δ 3.60), which in turn showed COSY coupling with H_2-3′ multiplet (δ 3.51).

The HRMS data of **10** suggested the molecular formula, $C_{23}H_{39}NO_3$. The ^{1}H and ^{13}C NMR data (Table 2) were similar to those of **9** with the replacement of the chlorinated terminal methylene C-3′ with a methyl group. The methyl triplet H_3-3′ (δ 1.11) was assigned based on its COSY coupling with H_2-2′ multiplet (δ 3.20).

The ^{1}H and ^{13}C NMR data of **11** (Table 2) indicated a monosubstituted benzene moiety replacing the methyl C-3′ in **10**. The broad methylene singlet H_2-2′ (δ 4.35) showed a ^{3}J-HMBC correlation with the aromatic proton doublet H-4′ and H-8′ (δ 7.26). The latter protons showed a COSY coupling with H-5′ and H-7′ doublet of doublets (δ 7.32), which in turn shows a COSY coupling with H-6′ (δ 7.27).

The antiproliferative activities of cembranoids **1** and **3**–**11** were evaluated against the human highly metastatic prostate cancer cell (PC-3M) growth using the 3-(4,5-dimethylthiazol-2-yl)-2,5-diphenyltetrazolium bromide (MTT) assays. Cembranoid **1** displayed little cytotoxic but potent antiproliferative effects at a dose of 10–20 nM, however it was cytotoxic at doses of 50 μM or higher (Fig. 1). Calcitonin (CT) is a potent endogenous growth factor for prostate cancer cells and exogenous addition of CT significantly increases proliferation and invasion of PC-3M cells.[25,26] Figure 1 also suggests that cembranoid **1** not only attenuated the basal growth of PC-3M cells, but almost abolished the CT-stimulated PC-3M cell proliferation. These effects of **1** were observed at all three periods of incubation (24, 48, and 72 h).

Table 2. ^{13}C and ^{1}H NMR Data of compounds **9**–**11**[a]

Position	**9**		**10**		**11**	
	δ_C	δ_H	δ_C	δ_H	δ_C	δ_H
1	46.1, CH	1.50, m	46.0, CH	1.55, m	46.1, CH	1.55, m
2	130.3, CH	5.17, dd (15.8, 9.2)	130.1, CH	5.16, dd (15.4, 9.2)	130.1, CH	5.16, dd (15.4, 8.8)
3	136.3, CH	5.36, d (15.8)	136.5, CH	5.36, d (15.4)	136.4, CH	5.37, d (15.4)
4	70.9, qC	—	70.8, qC	—	70.8, qC	—
5	51.4, CH_2	2.00, m	51.7, CH_2	2.05, m	51.6, CH_2	2.05, m
6	69.3, CH	5.60, dd (9.5, 9.0)	68.7, CH	5.57, dd (9.4, 9.0)	69.2, CH	5.62, dd (9.5, 9.1)
7	127.1, CH	5.27, d (9.9)	127.3, CH	5.24, d (9.9)	127.2, CH	5.24, d (9.9)
8	139.6, qC	—	139.3, qC	—	139.4, qC	—
9	38.9, CH_2	2.05, m 2.20, m	38.9, CH_2	2.10, m 2.25, m	38.9, CH_2	2.05, m 2.25, m
10	23.1, CH_2	2.10, m 2.20, m	23.1, CH_2	2.10, m	23.1, CH_2	2.10, m 2.30, m
11	124.0, CH	4.91, m	124.0, CH	4.91, m	124.0, CH	4.91, brt (5.2)
12	133.5, qC	—	133.5, qC	—	133.5, qC	—
13	36.5, CH_2	1.90, m 2.05, m	35.9, CH_2	1.90, m	36.5, CH_2	1.95, m 2.05, m
14	27.5, CH_2	1.25, m 1.60, m	27.4, CH_2	1.20, m 1.55, m	27.5, CH_2	1.25, m 1.60, m
15	33.2, CH	1.55, m	33.1, CH	1.50, m	33.2, CH	1.55, m
16	19.5, CH_3	0.79, d (6.6)	19.5, CH_3	0.79, d (6.6)	19.5, CH_3	0.77, d (6.6)
17	20.5, CH_3	0.82, d (6.6)	20.4, CH_3	0.80, d (6.6)	20.4, CH_3	0.82, d (6.6)
18	28.3, CH_3	1.36, s	28.2, CH_3	1.36, s	28.3, CH_3	1.36, s
19	16.0, CH_3	1.48, s	15.9, CH_3	1.48, s	16.0, CH_3	1.48, s
20	15.0, CH_3	1.72, s	15.0, CH_3	1.71, s	15.0, CH_3	1.73, s
1′	156.5, qC	—	156.6, qC	—	156.7, qC	—
2′	44.3, CH_2	3.60, m	36.5, CH_2	3.20, m	45.1, CH_2	4.35, brs
3′	42.8, CH_2	3.51, m	15.3, CH_3	1.11, t (7.0)	138.4, qC	—
4′, 8′					127.6, CH	7.26, 2H, d (8.0)
5′, 7′					128.8, CH	7.32, 2H, d (8.0, 7.8)
6′					127.7, CH	7.27, d (7.8)
–N*H*		5.09 brt, (6.0)		4.60, brs		4.98, brt (5.8)

[a] In $CDCl_3$, 400 MHz for ^{1}H and ^{13}C NMR. Coupling constants (*J*) are in Hz.

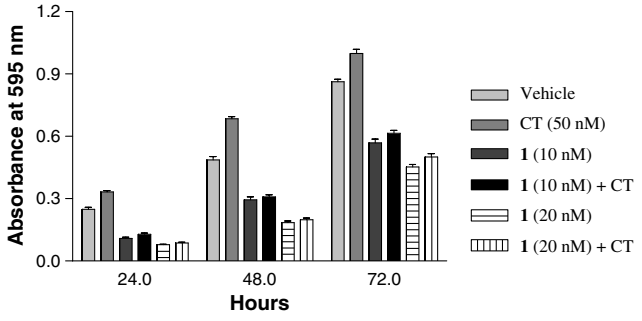

Figure 1. Antiproliferative and cytotoxic actions of **1** on PC-3M cells.

Cembranoid **1** showed a potent anti-invasive activity against PC-3M cells using Matrigel^{TM} assay (Fig. 2A and B). Figure 2A depicts the micrograph of invaded cells of each treatment group. The results show that the addition of CT observably increased the number of invaded cells. A dose of 5 nM of **1** caused an apparent decrease in the invasion of basal and CT-treated PC-3M cells. Figure 2B presents the pooled data of multiple experiments and suggests that CT caused twofold increase in the number of invaded cells. In contrast, **1** decreased basal as well as CT-treated PC-3M cells at a dose of 5 nM by two to threefold.

Recent evidence suggests that the destabilization of junctional complexes plays a crucial role in the progression of localized tumor to its metastatic form.[25,26] The strength of epithelial junctions can be assessed by the measurement of transepithelial resistance (TER) and paracellular permeability.[25,26] While TER can be measured by an ohm-meter, paracellular permeability is measured by the ability of Rhodamine-labeled antibodies (TRITC)-conjugated dextran through the cell layer of PC-3M cells.[25,26] Since cembranoid **1** inhibited the invasion of PC-3M cells in the Matrigel^{TM} model, testing whether this action was mediated by stabilization of junctional complexes was required. Therefore, the effect of **1** on TER and paracellular permeability of PC-3M cell cultures was tested. CT destabilizes junctional complexes of prostate cancer cells as characterized by a large reduction in TER and a marked increase in paracellular permeability of PC-3M cultures.[25] CT also increases the rate of cell proliferation, invasion and tumorigenicity.[25,26] Figure 3A presents TER of PC-3M cell layers at different time points after stimulation with and without CT. As expected, TER of PC-3M cell cultures increased with time. However, addition of 50 nM CT caused a dramatic reduction in TER (Fig. 3A). A dose of 50 nM of **1** did not affect baseline TER, but remarkably reduced CT-stimulated decrease in TER of PC-3M cells (Fig. 3A). Similar to decrease in TER, increase in paracellular permeability is also suggestive of junctional destabilization.[25] CT increased paracellular permeability of PC-3M cells (Fig. 3B). In contrast, **1** stabilized junctional complexes as suggested by the decrease of paracellular permeability of untreated and CT-treated PC-3M cells (Fig. 3B).

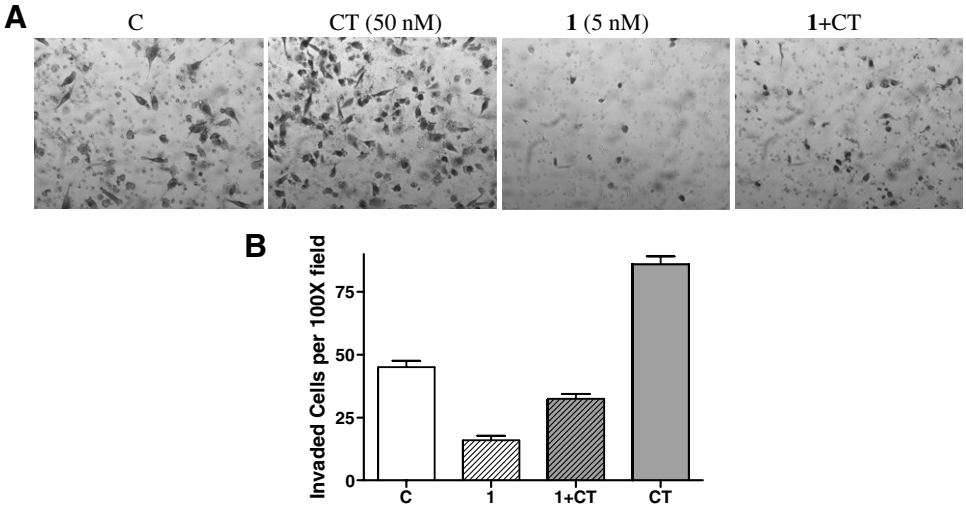

Figure 2. (A) Anti-invasive activity of β-diol (**1**) against PC-3M cells using Matrigel™ assay, Invaded cells/400X fields. (B) Quantification of invasion assay results.

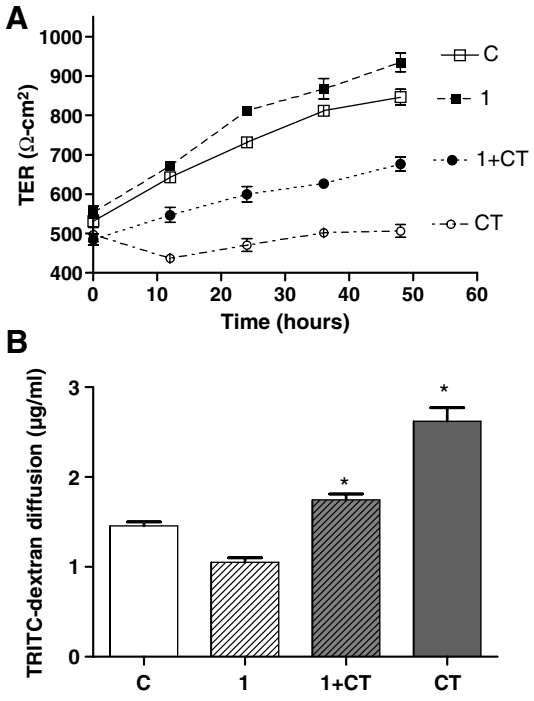

Figure 3. (A) Effect of 50 nM dose of **1** on transepithelial resistance of PC-3M cells. (B) Effect of **1** on paracellular permeability of PC-3M cells.

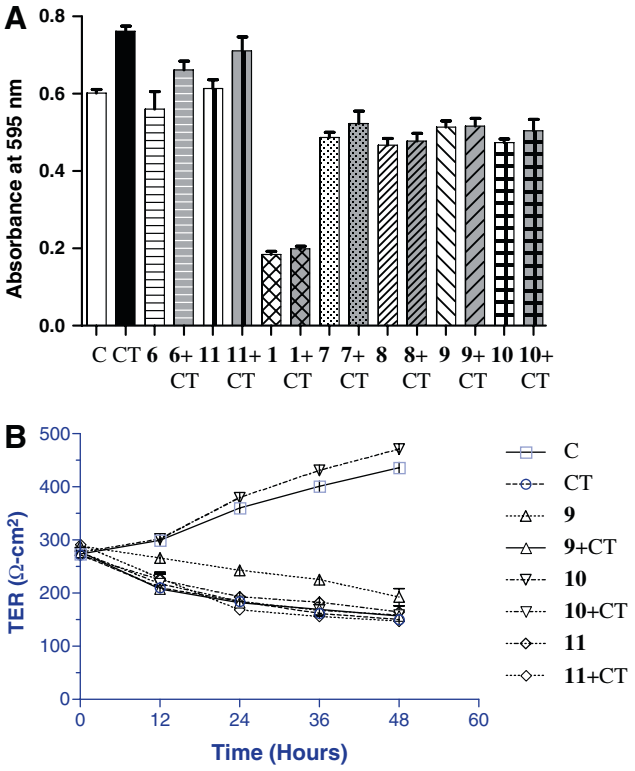

Figure 4. (A) Antiproliferative activity of 50 nM dose of cembranoids **6**–**11** against PC-3M cells using MTT assay. (B) Effect of carbamates**9**–**11** on transepithelial resistance of PC-3M cells.

Finally, the cytotoxic, antiproliferative, anti-invasive, and junction-stabilization effects of cembranoids **3**–**11** were evaluated (Fig. 4A and B). All compounds showed reduced toxicity compared to that of **1**. Biocatalytic products **6**–**8** also maintained the potent anti-invasive activity at 50 nM dose without cytotoxicity (Fig. 4A). Therefore, this is viewed as an excellent example of potential benefits of bioconversion in that while hydroxylation was stereoselectively achieved; the cytotoxicity of **1** was reduced, while the same anti-invasive potency of the parent compound was maintained. The carbamate analogs **9**–**11** also display potent antiproliferative activities against PC-3M cell line at treatment doses between 5 and 50 nM (Fig. 4A). Carbamate analogs **9**–**11** were much less cytotoxic than **1** at 50 nM dose in MTT assay (Fig. 4A). The effect of carbamate analogs **9**–**11** on baseline and CT-stimulated TER and paracellular permeability was examined (Fig. 4B). Only carbamate **10** stabilized junctional complexes, suggesting it may be a potential lead for future development as anti-metastatic drug for treatment of prostate cancer.

3. Conclusions

Biocatalysis of tobacco 2,7,11-cembratriene-4,6-diol (**1**) using the novel symbiotic *Bacilli* species afforded two new and four known hydroxylated metabolites **3**–**8**. The new C-6 carbamate analogs **9**–**11** were also prepared semisynthetically. Cembranoid **1** shows antiproliferative and anti-invasive activity against the human highly metastatic prostate PC-3M cancer cell line at 10–20 nM doses. A dose of 50 nM of **1** remarkably abolished CT-stimulated decrease in TER and increase of paracellular permeability of PC-3M cells. This indicates that **1** stabilized tight junctional complexes of PC-3M cells. Bioconversion and carbamate products showed similar potent anti-invasive activity at 50 nM dose without any sort of cytotoxicity. This is an example of a successful bioconversion, where the cytotoxic starting material bioconverted to less toxic metabolites while maintaining nearly the same anti-invasive potency. Cembranoids **1**, **6**–**8**, and **10** can be potential leads appropriate for future development as possible treatment for metastatic prostate cancers.

3.1. Experimental

3.1.1. General experimental procedures. Measurements of optical rotation were carried out on a Rudolph Research Analytical Autopol III polarimeter. IR spectra were recorded on a Varian 800 FT-IR spectrophotometer. The ^{1}H and ^{13}C NMR spectra were recorded in $CDCl_3$, using TMS as an internal standard, on a JEOL Eclipse NMR spectrometer operating at 400 MHz for ^{1}H and 100 MHz for ^{13}C. The HREIMS experiments were conducted at the University of Michigan on a Micromass LCT spectrometer. TLC analyses were carried out on precoated silica gel 60 F_{254} 500 μm TLC plates, using the developing system *n*-hexane/EtOAc (1:1) or $CHCl_3$/MeOH (9.5:0.5). For CC, silica gel 60 (particle size 63-200 μm) or Bakerbond octadecyl (C18), 40 μm was used.

3.1.2. Extraction and isolation. Fresh tobacco leaf powder (Custom Blends, NY, 27.2 kg) was extracted with hexane (130 L) in percolators three times at room temperature. The hexane extract was concentrated under vacuum and dried extract (1050 g) was vacuum liquid chromatographed on Silica gel (200–300 mesh, 2 Kg, Natland International Corporation) using gradient *n*-hexane/EtOAc to yield crude cembranoid-containing fraction (64.0 g) which was further chromatographed on normal phase and finally on reversed phase silica gel (MeOH–H_2O, 2:3, isocratic) to give **1** (3.6 g) and its C-4 epimer (17.9 g). The identity of **1** was confirmed by extensive NMR analysis and comparison with the literature.[1,2,5,11]

3.1.3. Symbiotic bacteria culture and isolation. About 2 g of each of frozen *N. magnifica* voucher, which was collected and kept frozen in sterile bags, was macerated overnight in 0.5 L Instant Ocean solution and then vacuum filter sterilized. Other 2 g of the sponge was aseptically blended in a sterile blender with 18 mL of the sponge Instant Ocean solution. Ten milliliters of 1/10, $1/10^2$, $1/10^3$, $1/10^4$, and $1/10^5$ serial dilutions were made using the previously prepared Instant Ocean solution. About 100 μl of each concentration was inoculated on the top of sterile tryptic soy or marine agar plates. Plates were incubated for 72–168 h at 28 °C. Symmetric fine colonies were separated and re-inoculated on corresponding agar media. Pure cultures were subjected to PCR analysis, DNA extraction (MO Bio Laboratories, Inc., Carlsbad, CA), and finally 16S rRNA sequencing.[22] Obtained alignments were subjected to Basic Local Alignment Search Tool (BLAST) queries. Identities of the isolated strains were based on partial 16S rRNA gene sequences. Strains had 16S rRNA gene sequence similarity $\geq$ 99% to the GenBank sequences listed below.

3.1.4. Biocatalysis. Biocatalytic studies were conducted as described elsewhere.[13,27] Thirty growing marine bacterial cultures were used for screening of **1**. These were: NB1: *Bacillus* sp. DF12 (AY462199), NC1: *B. megaterium* KL197 (AY030338), NA3: *Pelagiobacter variabilis* (AB167354), NC4: *Bacillus* sp. DF15 (AY462201), NC5: *Bacillus* sp. S/2 (AJ784847), NE1: *B. subtilis* BFAS (AY775778), SA2: *Bacillus* sp. KMM3737 (AY228462), SD1: *Halobacillus* sp. NT N168 (AB167053), NJ2: *Janibacter marinus* strain C6 (AY533561), 59A3: *Bacillus* sp. GSP11 (AY553069), NK6: *B. djibelorensis* (AF519467), NK8: *Bacillus* species Fa29 (AY131222), NK7: *Bacillus* species MT21 (AY690689), EA1: *B. pumilus* (AY112667), NG1A: *Microbacterium* sp. SKJH-23 (AY741722), NK4: *Bacillus* sp. EC2 (AY864632), EC2: *Pseudomonas* sp. C127 (DQ005892), SC1: Glacial ice bacterium G500K-17 (AF479334), SC3: *Pontibacillus marinus* BH030 (AY603977), SE2: *Oceanobacillus iheyensis* HTE831 (BA000028), SH1: *Micrococcus luteus* (AB079788), NF3: *B. subtilis* AX20 (AY825035), NK3: *Kocuria* sp. JL-72 (AY745813), SA6: *B. subtilis* MO2 (AY553095), 59D3: *B. acidogenesis* (AF547209), EF3: *Brevibacterium halotaleran* (AJ620368), EF1: *Virgiabacillus carmonensis* (AJ316302), EC2A: *Microbulbifer cystomdytense* (AJ620879), SK2: *Bacillus* sp. DF49 (AY462214), ED1: *B. megaterium* (AJ717381). These isolates show highest 16S rRNA gene sequence similarity to the sequences of these organisms in GenBank. GenBank accession numbers are listed in parenthesis. *Bacillus* sp. NC5, *B.* sp. NK8, and *B.* sp. NK7 were selected for biocatalysis scale-up of **1**. Each of these organisms was inoculated in twenty 1000-mL flasks each containing 250 mL tryptic soy or marine broth. After 48 h, compound **1** was added into their respective flasks (15 mg/flask). After 14 days, the growth medium was filtered and extracted with EtOAc (4×1000 mL). The EtOAc layer was then concentrated under vacuum. Residue obtained from biocatalysis of **1** by *Bacillus* species NC5 was purified on silica gel 60 column, followed by reversed phase Si gel medium pressure liquid chromatography (MPLC) to yield compound **3** (12 mg, R_f 0.26, $CHCl_3$/MeOH 9:1), compound **4** (4.5 mg, R_f 0.0.27, $CHCl_3$/MeOH 9:1), compound **5** (8 mg), and compound **6** (21 mg). *Bacillus* species NK8 fermentation extract was subjected to silica gel 60 column chromatography by *n*-hexane/EtOAc gradient elution followed by MPLC on C-18 reversed phase silica gel with isocratic

developing system MeOH/H_2O (1:2) to afford compound **7** (9 mg, R_f 0.32, $CHCl_3$/MeOH 9:1). Similarly, *Bacillus* species NK7 afforded compound **8** (11 mg, R_f 0.21, $CHCl_3$/MeOH 9:1).

3.1.5. Preparation of compounds 9–11. To solutions of **1** (16–35 mg) in toluene (2 mL), 10 μL of 2-chloroethyl isocyanate or 35 μL of ethyl isocyanate or 27 μL of benzyl isocyanate was added and separately mixed with 10 μL of Et_3N.[24] Each solution was separately stirred and refluxed for 3 h. Water was then added and the product of each reaction mixture was extracted with EtOAc.[24] Each EtOAc extract was dried over anhydrous Na_2SO_4 and concentrated under reduced pressure. Crude products were then purified by CC on silica gel (EtOAc-hexane 2:8 or 1:9) to give compounds **9**, 14 mg, 63%, **10**, 7.7 mg, 13%, and **11**, 20 mg, 39.8%, respectively.

3.1.6. Proliferation of PC-3M MTT assays. The growth of prostate cell line PC-3M was measured by MTT kit (ATCC). Exponentially growing cells were plated in a 96-well plate at a density of 8×10^3 cells per well and allowed to attach for 24 h. Complete growth medium was replaced with 100 μL of RPMI serum-free medium (GIBCO-Invitrogen, NY) and culture continued at 37 °C under 5% CO_2. After 24 h of culture, the cells were treated with MTT solution at 37 °C for 4 h.[24,25] The color reaction was stopped by the addition of solubilization/stop solution (100 μL/well), and the incubation at 37 °C continued to completely dissolve the formazan product. Absorbance of the samples was determined at 595 nm with an ELISA plate reader (Bio-Rad, Hercules, CA).

3.1.7. Invasion assay. These experiments were conducted in 24-well, two compartmented, Matrigel™ invasion chambers (Becton Dickinson, Bedford, MA).[25,26] Exponentially growing prostate cancer cell line was serum-starved for 24 h with basal RPMI medium containing no serum or growth factors (but containing 0.1% BSA, 10 mM Hepes, 4 mM L-glutamine, 100 IU/mL penicillin G, and 100 mg/mL streptomycin). The cells were then harvested and seeded at a density of 25×10^3 cells/well in the upper insert of the Matrigel™ invasion chamber. The lower chamber received the chemo-attractant medium, which consisted of 90% basal RPMI medium and 10% conditioned medium from the cultures of PC-3 M cells constitutively expressing active Gas protein. The incubations were carried out for 24 h, after which the Matrigel™ (along with non-invading cells) was scraped off with cotton swabs, and outer side of the insert was fixed and stained using Diff Quick staining (Dade Behring Diagnostics, Aguada, Peurto Rico). The number of cells migrated on the outer bottom side of the insert was counted under the microscope in six or more randomly selected fields (magnification: 100×). The final results were expressed as means ± SEM per 100× field. Each experiment was conducted in triplicates, and the experiment was repeated twice.[25,26]

3.1.8. Growth correction. Since some of tumor cell lines exhibit high proliferation rate, it is likely that the cells migrated during early part of the 24 h incubation period could proliferate during the remaining period of incubation, leading to a slight overestimation of the final results. To correct this probability, the growth rate of PC-3M cells was determined under identical culture conditions. 25×10^3 cells were plated at hourly intervals in six-well dishes and cultured with/without CT (50 nM) for 1–24 h. Mean percent increase in the cell number was determined at the end of the incubation period by counting the net increase in the number of cells. The relative CT-induced increase of the pooled results of all time points was found to be 1.19 (vehicle control = 1). This correction was applied to the results of invasion assays.[25,26]

3.1.9. Measurement of transepithelial resistance. Cells were plated at confluency and grown on six well Transwell filters (0.4 μm pore size) in complete medium. TER values were measured in duplicate wells in every 12 h using EVOM voltohmmeter (World Precision Instruments). The TER values were normalized to the area of the monolayer filter and calculated by subtracting the blank values from the filter and bathing medium. All cell culture media were supplemented with 25 mM Hepes, pH 7.4, and the integrity and cell density of monolayers were carefully monitored during TER measurement studies.[25,26]

3.1.10. Permeability assay (paracellular diffusion of dextran). Cells were plated at confluency and grown on 12-well Transwell filters in complete medium for optimum TER development. Tetramethyl-rhodamine-dextran, with an average molecular mass of 4 kDa (Sigma, St. Louis, MO) dissolved in Hanks' Balanced Salt Solution (HBSS) to a concentration of 1 mg/mL, was added to the upper chamber. The lower chamber was replaced with HBSS. At various time intervals, 100 μL aliquots were collected from the lower chamber and luminescence assayed using spectrophotometer using excitation 530 and emission 590.[25,26]

3.1.11. (1*S*,2*E*,4*R*,6*R*,7*Z*,11*E*)-2,7,11-cembratriene-4,6,19-triol (3). Colorless oil, $[\alpha]_D^{25}$ +58.2 (*c* 0.1, $CHCl_3$); IR υ_{max} ($CHCl_3$) 3602, 3420, 2928, 2856, 1462, 1379, 1082, 908 cm^{-1}; ^1H and ^{13}C NMR, see Table 1; HREIMS *m*/*z* 345.2395 $[M+Na]^+$ (calcd for $C_{20}H_{34}O_3Na$, 345.2406).

3.1.12. (1*S*,2*E*,4*R*,6*R*,7*E*,9*S*,11*E*)-2,7,11-cembratriene-4,6,9-triol (4). Colorless oil, $[\alpha]_D^{25}$ +68.0 (*c* 0.1, $CHCl_3$); IR υ_{max} ($CHCl_3$) 3421, 2930, 2855, 1461, 1374, 1096, 907 cm^{-1}; ^1H and ^{13}C NMR, see Table 1; HRESMS *m*/*z* 345.2438 $[M+Na]^+$ (calcd for $C_{20}H_{34}O_3Na$, 345.2406).

3.1.13. Compound 9. Colorless oil; $[\alpha]_D^{25}$ +58.9 (*c* 0.50, $CHCl_3$); IR ν_{max} (neat) 3685, 3612, 3450, 3020, 2929, 1703, 1513, 1428, 1221, 1045 cm^{-1}; ^1H and ^{13}C NMR see Table 2; HRESMS *m*/*z* 434.2427 $[M+Na]^+$ (calcd for $C_{23}H_{38}ClNO_3Na$, 434.2438).

3.1.14. Compound 10. Colorless oil; $[\alpha]_D^{25}$ +50.3 (*c* 0.06, $CHCl_3$); IR ν_{max} (neat) 3685, 3450, 3021, 2928, 1966, 1602, 1518, 1425, 1213 cm^{-1}; ^1H and ^{13}C NMR see Ta-

ble 2; HRESMS *m/z* 400.2830 $[M+Na]^+$ (calcd for $C_{23}H_{39}NO_3Na$, 400.2828).

3.1.15. Compound 11. Yellowish oil; $[\alpha]_D^{25}$ +52.1 (*c* 0.60, $CHCl_3$); IR ν_{max} (neat) 3449, 2929, 1711, 1511, 1455, 1259, 1127 cm^{-1}; ^1H and ^{13}C NMR see Table 2; HRESMS *m/z* 462.2975 $[M+Na]^+$ (calcd for $C_{28}H_{41}NO_3Na$, 462.2984).

Acknowledgments

This publication was made possible by the support of Philip Morris USA Inc. and Philip Morris International as well as the NIH Grant No. P20RR16456 from the BRIN Program of the National Center for Research Resources and R01 Grant No. R01CA96534 (G.V.S.). Its contents are solely the responsibility of the authors and do not necessarily represent the official views of NIH. FAR and DB were supported by the Governor's Biotechnology Initiative of the Louisiana Board of Regents (BOR#021-Moving an Established Marine Biotechnology Program to the Next Level: Natural Product Screening and Development). Louisiana Board of Regents is also acknowledged for the support of the NMR spectrometer probe purchase (LEQSF (2007–08)-ENH-TR 80 to KAE).

References and notes

1. Wahlberg, I.; Enzell, C. R. *Beitrage zur Tabakforschung International* **1984**, *12*, 93.
2. Wahlberg, I.; Eklund, A. M. In *Trends in Flavour Research*; Maarse, H., Heji, V., Eds.; Elsevier Science B.V.: Oxford, UK, 1994; pp 449–462.
3. Wahlberg, I.; Forsblom; Vogt, C.; Eklund, A. M.; Nishida, T.; Enzell, C. R.; Berg, J. E. *J. Org. Chem.* **1985**, *5*, 4527.
4. Dauben, W. G.; Thiessen, W. E.; Resnick, P. R. *J. Am. Chem. Soc.* **1962**, *84*, 2015.
5. Wahlberg, I.; Olsson, E.; Berg, J. E. In *Prog. Flavour Precursor Stud. Proc. Int. Conf.*, Schreier, P., Winterhalter, P., Eds; Allured Publishing Corporation: Carol Stream, Illinois, 1993; pp 83–95.
6. Ferchmin, P. A.; Hao, J.; Perez, D.; Penzo, M.; Maldonado, H. M.; Gonzalez, M. T.; Rodriguez, A. D.; Jean, D. V. *J. Neurosci. Res.* **2005**, *82*, 631.
7. Olsson, E.; Holth, A.; Kumlin, E.; Bohlin, L.; Wahlberg, I. *Planta Medica* **1993**, *59*, 293.
8. Saito, Y.; Takayawa, H.; Konishi, S.; Yoshida, D.; Mizusaki, S. *Carcinogenesis* **1985**, *6*, 1189.
9. Saito, Y.; Nishino, H.; Yoshida, D.; Mizusaki, S.; Ohnishi, A. *Oncology* **1988**, *45*, 122.
10. Saito, Y.; Tsujino, Y.; Kaneko, H.; Yoshida, D.; Mizusaki, S. *Agric. Biol. Chem.* **1987**, *51*, 941.
11. Wahlberg, I.; Eklund, A. M.. In *Progress in the Chemistry of Organic Natural Products*; Herz, W., Kirby, G. W., Moore, R. E., Steglich, W., Tamm, C. H., Eds.; Springer-Verlag Wien: New York, 1992; Vol. 59, pp 142–293.
12. ElSayed, K. A.; Sylvester, P. W. *Drugs* **2007**, *16*, 877.
13. Clark, A. M.; McChesney, J. D.; Hufford, C. D. *Med. Res. Rev.* **1985**, *5*, 231.
14. Thayer, A. N. *Chem. Eng. News* **2006**, *84*, 16.
15. Sanchez-Porro, C.; Martin, S.; Mellado, E.; Ventosa, A. *J. Appl. Microbiol.* **2003**, *94*, 295.
16. Fukano, Y.; Ito, M. *Appl. Environ. Microbiol.* **1997**, *63*, 1861.
17. Yamazaki, Y.; Mikami, Y. Jpn. Kokai Tokkyo Koho 85-266107, 1987; Yamazaki, Y.; Mikami, Y. *Chem. Abstr.* **1987**, *110*, 132381.
18. Yamazaki, Y.; Mikami, Y. Jpn. Kokai Tokkyo Koho 86-72567, 1987; Yamazaki, Y.; Mikami *Chem. Abstr.* **1987**, *110*, 111980.
19. Arnarp, J.; Chu, W. L. A.; Enzell, C. R.; Hewitt, G. M.; Kutney, J. P.; Li, K.; Milanova, R. K.; Nakata, H.; Nasiri, A.; Okada, Y. *Acta Chem. Scand.* **1993**, *47*, 683.
20. Arnarp, J.; Chu, A. W. L.; Enzell, C. R.; Hewitt, G. M.; Kutney, J. P.; Li, K.; Milanova, R. K.; Nakata, H.; Nasiri, A.; Tsuda, T. *Acta Chem. Scand.* **1993**, *47*, 689.
21. Arnarp, J.; Chu, A. W. L.; Enzell, C. R.; Hewitt, G. M.; Kutney, J. P.; Li, K.; Milanova, R. K.; Nakata, H.; Nasiri, A.; Tsuda, T. *Acta Chem. Scand.* **1993**, *47*, 793.
22. Rainey, F. A.; Ward-Rainey, N.; Kroppenstedt, R. M.; Stackebrandt, E. *Int. J. Systematic Bacteriol.* **1996**, *46*, 1088.
23. Forsblom, I.; Berg, J. E.; Wahlberg, I. *Acta Chem. Scand.* **1993**, *47*, 80.
24. Basheer, A.; Rappoport, Z. *J. Org. Chem.* **2006**, *71*, 9743.
25. Sabbisetti, V. S.; Chirugupati, S.; Thomas, S.; Vaidya, K. S.; Reardon, D.; Chiriva-Internati, M.; Iczkowski, K. A.; Shah, G. V. *Int. J. Cancer* **2005**, *117*, 551.
26. Shah, G. V.; Rayford, W.; Noble, M. J.; Austenfeld, M.; Weigel, J.; Vamos, S.; Mebust, W. K. *Endocrinology* **1994**, *134*, 596.
27. El Sayed, K. A.; Hamann, M. T.; Waddling, C. A.; Jensen, C.; Lee, S. K.; Dunstan, C. A.; Pezzuto, J. M. *J. Org. Chem.* **1998**, *63*, 7449.